



XRCC3 polymorphism is associated with hypertension-induced left ventricular hypertrophy

Andi Ariyandy¹ · Chiemi Sakai¹ · Mari Ishida¹ · Ryusei Mizuta¹ · Kiyoshi Miyagawa² · Satoshi Tashiro³ · Aiko Kinomura³ · Koji Hiraaki⁴ · Keitaro Ueda¹ · Masao Yoshizumi¹ · Takafumi Ishida⁵

Received: 21 November 2017 / Revised: 13 December 2017 / Accepted: 13 December 2017 / Published online: 6 April 2018
© The Japanese Society of Hypertension 2018

Abstract

Deficiency of X-ray repair cross-complementing protein 3 (XRCC3), a DNA-damage repair molecule, and the 241Met variant of XRCC3 have been reported to increase endoreduplication, which induces polyploidy. The aims of this study were to determine the impact of the XRCC3 polymorphism on the incidence of hypertension-induced left ventricular hypertrophy (LVH) and to investigate the mechanisms underlying any potential relationship. Patients undergoing chronic hemodialysis ($n = 77$) were genotyped to assess for the XRCC3 Thr241Met polymorphism. The XRCC3 241Thr/Met genotype was more frequent in the LVH (+) group than in the LVH (−) group (42.3 vs. 13.7%, $\chi^2 = 7.85$, $p = 0.0051$). To investigate possible mechanisms underlying these observations, human XRCC3 cDNA of 241Thr or that of 241Met was introduced into cultured CHO cells. The surface area of CHO cells expressing XRCC3 241Met was larger than that expressing 241Thr. Spontaneous DNA double-strand breaks accumulated to a greater degree in NIH3T3 cells expressing 241Met (3T3-241Met) than in those expressing 241Thr (3T3-241Thr). DNA damage caused by radiation induced cell senescence more frequently in 3T3-241Met. The levels of basal and TNF- α -stimulated MCP-1 mRNA and protein secretion were higher in 3T3-241Met. Finally, FACS analysis revealed that the cell percentage in G2/M phase including polyploidy was significantly higher in 3T3-241Met than in 3T3-241Thr. Furthermore, the basal level of MCP-1 mRNA positively correlated with the cell percentage in G2/M phase and polyploidy. These data suggest that the XRCC3 241Met increases the risk of LVH via accumulation of DNA damage, thereby altering cell cycle progression and inducing cell senescence and a proinflammatory phenotype.

These authors contributed equally: Andi Ariyandy, Chiemi Sakai, Mari Ishida.

Electronic supplementary material The online version of this article (<https://doi.org/10.1038/s41440-018-0038-0>) contains supplementary material, which is available to authorized users.

✉ Mari Ishida
mari@hiroshima-u.ac.jp

¹ Department of Cardiovascular Physiology and Medicine, Hiroshima University, Hiroshima, Japan

² Laboratory of Molecular Radiology, Center for Disease Biology and Integrative Medicine, Graduate School of Medicine, The University of Tokyo, Tokyo, Japan

³ Research Institute for Radiation Biology and Medicine, Hiroshima University, Hiroshima, Japan

⁴ Minamikaita Hospital, Hiroshima, Japan

⁵ Department of Cardiovascular Medicine, Fukushima Medical University, Fukushima, Japan

Introduction

Left ventricular hypertrophy (LVH) involves structural remodeling of the heart in response to pressure overload. Previous studies have shown that the occurrence of LVH does not solely depend on the duration or severity of hypertension and that not all hypertensive patients develop LVH [1]. The ability to determine an individual's susceptibility to LVH is clinically important, as the risk of cardiovascular morbidity and mortality in hypertensive patients with LVH is increased two-to-four-fold when compared with patients without LVH [1]. Previous studies have demonstrated that LVH is mediated by the mechanical stress of pressure overload, neurohormonal factors, and various genetic factors that independently exert trophic effects on myocytes and non-myocytes in the heart [2]. Single nucleotide polymorphisms (SNPs) of some candidate genes, such as those encoding for angiotensin-converting enzyme, angiotensinogen, or the

angiotensin II type I receptor, have been shown to be associated with LVH [2].

X-ray repair cross-complementing protein 3 (XRCC3) participates in homologous recombination and is involved in the repair pathway for double-strand breaks (DSBs). We previously reported that XRCC3 deficiency results in a defect in recombination and results in increased endoreduplication [3]. Endoreduplication is the replication of the nuclear genome without subsequent cell division; this process leads to polyploidy and an increase in cell size. A single nucleotide polymorphism (C18067T, rs861539) in exon 7 of the XRCC3 gene results in the amino acid change (threonine to methionine) at codon 241 (Thr241Met) [4]. We have also shown that cells with the Thr241Met mutation undergo endoreduplication [3].

LVH is associated with an increased risk of major cardiovascular events and all-cause mortality in hypertensive patients. Further, LVH is a common problem in patients undergoing chronic HD, because interdialytic volume overload induces continuous hypertension. Thus, we investigated whether the XRCC3 polymorphism is associated with hypertension-induced LVH in HD patients and attempted to characterize the molecular mechanisms for the association between the XRCC3 polymorphism and LVH.

Materials and methods

Patients

Seventy-seven hypertensive patients (52 males, 25 females; mean age, 67.8 ± 11.9 years) with renal failure undergoing chronic HD were studied. Systolic blood pressure (SBP) and diastolic blood pressure (DBP) were measured in the supine position before and after each dialysis session and values from 3 different sessions were averaged. Body mass index (BMI) at the end of dialysis and body weight gain between dialysis were also determined. Two-dimensional-controlled M-mode echocardiograms were recorded after hemodialysis session, and LVH was diagnosed if the wall thickness of both the interventricular septum and the left ventricular (LV) posterior wall were more than 12 mm [5]. The study was approved by the Ethics Committee of Hiroshima University for Human Genome and Genetic Sequencing Research, and written informed consent was obtained from all patients according to the Declaration of Helsinki.

Determination of genotypes

Genomic DNA was extracted from peripheral blood leukocytes by using NucleoSpin Blood (Macherey-Nagel, Germany). XRCC3 codon 241 genotypes were determined by

polymerase chain reaction (PCR) and restriction fragment length polymorphism (RFLP). We amplified the XRCC3 polymorphic site from ~100 ng of genomic DNA using 0.3 $\mu\text{mol/L}$ of the forward primer (5'-TTGGGGCCTCTTTGAGA-3), 0.3 $\mu\text{mol/L}$ of the reverse primer (5'-AACGGCTGAGGGTCTTCT-3), 0.4 mmol/L of deoxynucleotide triphosphates (dNTPs), and 1.0 unit of KOD FX DNA polymerase from TOYOBO (Japan). The PCR reactions were carried out in DNAEngine Thermal Cycler (Bio-Rad, Hercules CA, USA) with an initial denature step of 2 min at 94 °C, followed by 30 cycles of denature at 98 °C for 10 s, annealing at 58 °C for 30 s, and extension at 68 °C for 1 min. The PCR products were digested with N1aIII (New England Biolabs, Ipswich, MA, USA) and resolved in 3% agarose gels (Nippon Gene, Japan). Three possible genotypes were defined depending on the banding patterns: Thr/Thr (240 and 315 bp), Thr/Met (107, 208, 240, and 315 bp), and Met/Met (107, 208, and 240 bp) [4].

Cell culture

Chinese hamster ovary (CHO)-K1 cells (ATCC, Manassas, VA) were maintained in Dulbecco's Modified Eagle Medium (DMEM)-F12 with 5% fetal calf serum (FCS), and the mouse NIH3T3 fibroblast cell line was maintained in DMEM with 10% FCS at 37 °C in a 5% CO₂ humidified incubator.

Determination of cell size

Human XRCC3 cDNAs were inserted into the pMMTV vector with a zeocin resistance gene. CHO cells were grown to 70–80% confluence and then transiently transfected either with 3 μg of pMMTV, human XRCC3 cDNA of 241Thr in pMMTV, or that of 241Met in pMMTV together with 1 μg of lacZ using Lipofectamine 2000 reagent (Thermo Fisher Scientific, Waltham, MA). The cells were incubated for 4–6 h at 37 °C in a CO₂ incubator, followed by overnight recovery with DMEM/F12 containing 5% FCS. After an additional 24 h of incubation, the cells were subjected to X-gal staining for the assessment of cell size. The cell surface area was analyzed by Image J software version 1.4.

Stable transfection in NIH3T3 cells

The NIH3T3 cells were transfected either with empty vector, pMMTV, human XRCC3 cDNA of 241Thr in pMMTV, or that of 241Met in pMMTV using Lipofectamine 2000 reagent (Thermo Fisher Scientific, Waltham, MA). Transfected cells were cultured with DMEM/10% FCS containing 400 $\mu\text{g/ml}$ of zeocin for selection. Ten colonies were selected in each group. The expression of human XRCC3 in transfected NIH3T3 cells was confirmed by western blot analysis (Supplementary Figure 1).

Table 1 Baseline characteristics of the patients: comparison between LVH(-) and LVH(+)

	LVH(-) (n = 51)	LVH(+) (n = 26)	P-value
Male/Female (n)	34/17	18/8	0.82
Age (years)	67.3 ± 10.1	68.8 ± 15.4	0.76
Body Mass Index (kg/m ²)	20.6 ± 2.5	23.8 ± 3.0	0.001 ^a
Intradialytic body weight gain (kg)	1.7 ± 1.1	2.0 ± 0.9	0.21
Duration from HD introduction (years)	7.3 ± 7.4	3.3 ± 2.8	0.12
SBP before HD (mmHg)	147.3 ± 20.3	154.9 ± 18.5	0.12
DBP before HD (mmHg)	63.7 ± 7.2	65.9 ± 6.7	0.23
SBP after HD (mmHg)	148.7 ± 23.3	148.7 ± 14.7	0.65
DBP after HD (mmHg)	66.4 ± 7.2	66.2 ± 5.0	0.66
LV septal wall thickness (mm)	10.7 ± 1.4	13.0 ± 0.8	<0.001 ^a
LV posterior wall thickness (mm)	11.0 ± 1.4	13.9 ± 1.5	<0.001 ^a
LV end-diastolic dimension (mm)	44.7 ± 7.5	45.9 ± 7.0	0.52
LV end-systolic dimension (mm)	29.1 ± 7.7	28.9 ± 6.2	0.97
LA dimension (mm)	38.9 ± 6.2	41.5 ± 5.4	0.059
LV ejection fraction (%)	64.0 ± 12.0	65.7 ± 9.2	0.66
LV fractional shortening (%)	36.3 ± 7.8	37.2 ± 7.3	0.65
Thr241Met genotype, n (%)	7 (13.7)	11 (42.3)	0.005 ^a

LVH left ventricular hypertrophy, HD hemodialysis, SBP systolic blood pressure, DBP diastolic blood pressure, LV left ventricular, LA left atrial

^a Indicates statistical significance

Detection of DSBs

DSBs were detected by immunofluorescent analysis using the anti-53BP1 antibody. Cells were fixed with 4% paraformaldehyde and permeabilized with Triton X-100. The cells were incubated with anti-53BP1 antibody for 30 min at 37 °C and then with Cy3-conjugated secondary antibody for 30 min at 37 °C. Nuclei were stained with 4',6-diamidino-2-phenylindole (DAPI). All images of slides were obtained automatically with a CoolCube1 camera, mounted with MetaSystems (MetaSystems Hard & Software GmbH, Altlussheim, Germany), and analyzed by Metafer classifier (MetaSystems). Foci in about 4000 nuclei were counted.

Senescence-associated β-galactosidase (SA β-gal) staining

Cell senescence was detected by SA β-gal staining using a senescence cell staining kit (Sigma-Aldrich, St. Louis, MO, USA) according to the manufacturer's protocol. To

calculate the percentage of SA β-gal positive cells, at least 500 cells were counted for each sample.

Real-time PCR (RT-PCR)

Total RNA was isolated from the cells using TRIzol reagent (Invitrogen, Carlsbad, CA). Quantitative RT-PCR was carried out using the Thunderbird qRT-PCR Kit with SYBR Green (TOYOBO) and CFX96 real-time PCR system (Bio-Rad Laboratories, Hercules, CA) according to the manufacturer's instructions. The following primers were purchased from Takara Biomedics (Tokyo, Japan): interleukin-6 (IL-6; NM_031168.1), forward 5'-CAACGATGATGCACTTGCAGA-3' and reverse 5'-CTCCAGGTAGCTATGGTACTCCAGA-3'; IL-8 (NM_011339.2), forward 5'-CTCCTGCTGGCTGTCCTAAC-3' and reverse 5'-CCTGAATACACAGACATCGTAGCTC-3'; and MCP-1 (NM_011333.3), forward 5'-AGCAGCAGGTGTCCCAAAGA-3' and reverse 5'-GTGCTGAAGACCTTAGGGCAGA-3'. 18S rRNA was used as the housekeeping gene.

Quantification of MCP-1 protein secretion

To quantify secreted MCP-1 protein in culture media, we used a solid-phase ELISA following the manufacturer's protocol (Mouse CCL2/JE/MCP-1 Quantikine ELISA kit, R&D Systems, Minneapolis, MN).

Flow cytometry analysis

The NIH3T3 cells were harvested and fixed with 70% cold ethanol at 4 °C for 30 min. After being washed in phosphate-buffered saline (PBS), the cells were incubated in propidium iodide (PI) /RNase staining buffer (BD Pharmingen, Franklin Lakes, NJ) at room temperature for 15 min. Then, the samples were analyzed by FACSCalibur flow cytometry (Becton Dickinson, Franklin Lakes, NJ), and the cell cycle distributions were analyzed by Flowjo software (Verity Software House, Topsham, ME, USA).

Statistics

For clinical data, variables are expressed as means ± standard deviation or as percentages. Intergroup differences were compared using Mann-Whitney's *U*-test. Differences in the distribution of alleles and genotypes between the groups were analyzed by the Chi-Square test. Odd ratios (ORs) and the corresponding 95% confidence intervals (CIs) were computed with Statistical Package of Social Science Software program, version 21 (IBM, Armonk, NY, USA). Logistic regression models were fitted.

Table 2 Distribution of genotype and allele frequencies in LVH(−) and LVH(+) patients and the association between LVH and XRCC3 polymorphism

XRCC3	n	Genotype frequencies (n (%))			Thr/Thr vs. Thr/Met			Allele frequencies (%)		Thr vs. Met		
		Thr/Thr (%)	Thr/Met (%)	Met/Met (%)	χ^2	P	OR (95% CI)	Thr	Met	χ^2	P	OR (95% CI)
Total	77	59 (76.6)	18 (23.4)	0				88.31	11.69			
LVH(−)	51	44 (86.3)	7 (13.7)	0	7.85	0.0051 ^a	4.61	93.14	6.86	6.8	0.009 ^a	3.64
LVH(+)	26	15 (57.7)	11 (42.3)	0			(1.51–14.05)	78.85	21.15			(1.32–10.06)

LVH left ventricular hypertrophy, OR odds ratio

^aIndicates statistical significance based on the Chi-Square test

For in vitro data, variables are expressed as means \pm standard error. The Kruskal–Wallis test or one-way ANOVA test was conducted followed by a Bonferroni's multiple comparisons test. Relationships between variables were assessed using Spearman's rank correlation coefficient. Statistical analyses were performed using Statcel3 (OMS, Japan).

Results

Patient study

Seventy-seven hypertensive patients with renal failure undergoing chronic HD were studied. Hypertension is very common in patients undergoing dialysis, and LVH is one of the most common cardiovascular problems in HD patients [6, 7]. Twenty-six of 77 patients (30.7%) were found to have LVH. No significant difference was found in gender, age, interdialytic body weight gain, duration from initiation of first HD treatment, SBP before and after HD, or DBP before and after HD when comparing patients without LVH (LVH(−)) and those with LVH (LVH(+)) (Table 1).

The distributions of XRCC3 Thr241Met genotypes and allele frequencies of all patients are shown in Table 2. No statistical difference was found in age, BMI, interdialytic body weight gain, SBP before and after HD, and DBP before and after HD when comparing the Thr/Thr and Thr/Met genotype (Table 3). The LV posterior wall was thicker in Thr/Met than in Thr/Thr. The distribution of the XRCC3 Thr241Met genotypes was in Hardy–Weinberg equilibrium in all patients ($\chi^2 = 1.34$, $p = 0.25$), and both LVH(−) ($\chi^2 = 0.28$, $p = 0.60$) and LVH(+) group ($\chi^2 = 1.87$, $p = 0.17$) (Table 2). The distribution of the XRCC3 Thr241Met genotypes and the allele frequency were shown in Table 2. There were significant differences in genotype distribution ($\chi^2 = 7.85$, $p = 0.0051$) and in allele frequency distribution ($\chi^2 = 6.80$, $p = 0.009$) when comparing the LVH(+) group and the LVH(−) group. The risk of LVH was increased in Thr/Met patients when compared with Thr/

Table 3 Baseline characteristics of the patients: Comparison between genotypes

	Thr/Thr (n = 59)	Thr/Met (n = 18)	P-value
Male/Female (n)	42/17	10/8	0.215
Age (years)	65.7 \pm 14.8	69.7 \pm 16.0	0.567
Body Mass Index (kg/m ²)	21.9 \pm 3.2	20.7 \pm 2.3	0.431
Intradialytic weight gain (kg)	1.8 \pm 1.0	2.0 \pm 0.9	0.35
Duration from HD introduction (years)	5.7 \pm 6.3	7.0 \pm 7.0	0.437
SBP before HD (mmHg)	150.4 \pm 21.6	147.8 \pm 12.7	0.942
DBP before HD (mmHg)	64.2 \pm 6.9	65.2 \pm 7.8	0.625
SBP after HD (mmHg)	149.7 \pm 22.2	145.3 \pm 14.4	0.602
DBP after HD (mmHg)	66.7 \pm 7.0	65.3 \pm 4.3	0.693
LV septal wall thickness (mm)	11.4 \pm 1.6	11.9 \pm 1.7	0.16
LV posterior wall thickness (mm)	11.7 \pm 1.9	12.8 \pm 2.2*	0.045 ^a
LV end-diastolic dimension (mm)	45.2 \pm 7.9	44.9 \pm 5.1	0.934
LV end-systolic dimension (mm)	29.4 \pm 7.7	27.6 \pm 4.1	0.4
LA dimension (mm)	39.6 \pm 6.3	40.5 \pm 4.9	0.424
LV ejection fraction (%)	63.8 \pm 11.8	67.6 \pm 7.4	0.448
LV fractional shortening (%)	36.4 \pm 8.2	37.5 \pm 4.4	0.858

HD hemodialysis, SBP systolic blood pressure, DBP diastolic blood pressure, LV left ventricular, LA left atrial

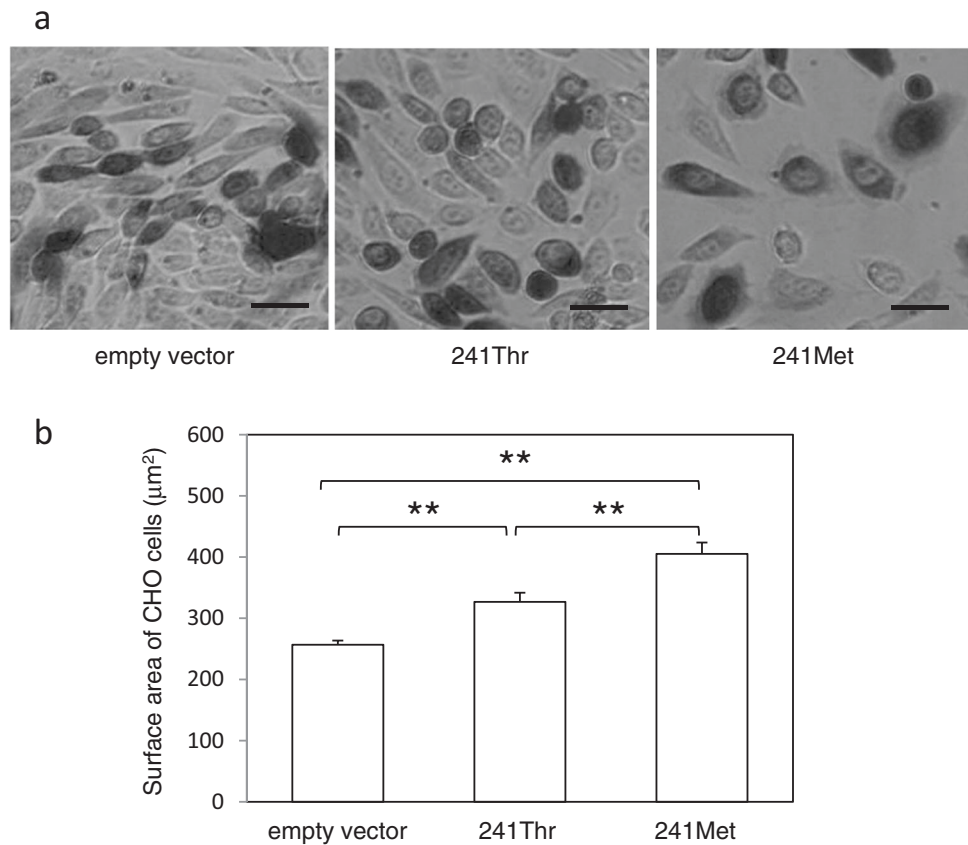
^aIndicates statistical significance

Thr patients (OR = 4.61; 95% CI, 1.51–14.05; $P = 0.005$) (Table 2).

In vitro experiments

We investigated the possible molecular mechanisms by which the Met allele results in LVH. We first examined whether the XRCC3 241Met variant induced cell hypertrophy. CHO-K1 cells were transiently transfected either with pMMTV, human XRCC3 cDNA of 241Thr or that of

Fig. 1 Induction of XRCC3 241Met increases cell size. **a** Representative appearance of Chinese hamster ovary (CHO) cells transfected with pMMTV containing no insert (empty vector), 241Thr or 241Met, along with the LacZ reporter gene (scale bars of 30 μm). **b** Cell surface area of CHO cells. CHO cells were transiently transfected with pMMTV containing no insert (empty vector), 241Thr or 241Met, along with the LacZ reporter gene. At least 100 cells were analyzed in one experiment, and the experiments were repeated four times. $**P < 0.01$. A full color version of this figure is available at the *Hypertension Research* journal online



241Met together with lacZ, and cell surface area of transfected cells was analyzed. CHO-K1 cells with the XRCC3 241Met variant were larger than those with the 241Thr variant (mean \pm standard error [μm^2]: pMMTV, 256.7 ± 6.9 ; XRCC3 241Thr, 326.73 ± 15.0 ; XRCC3 241Met, 405.1 ± 18.6 ; Fig. 1a, b), indicating that the XRCC3 241Met variant induces cell hypertrophy.

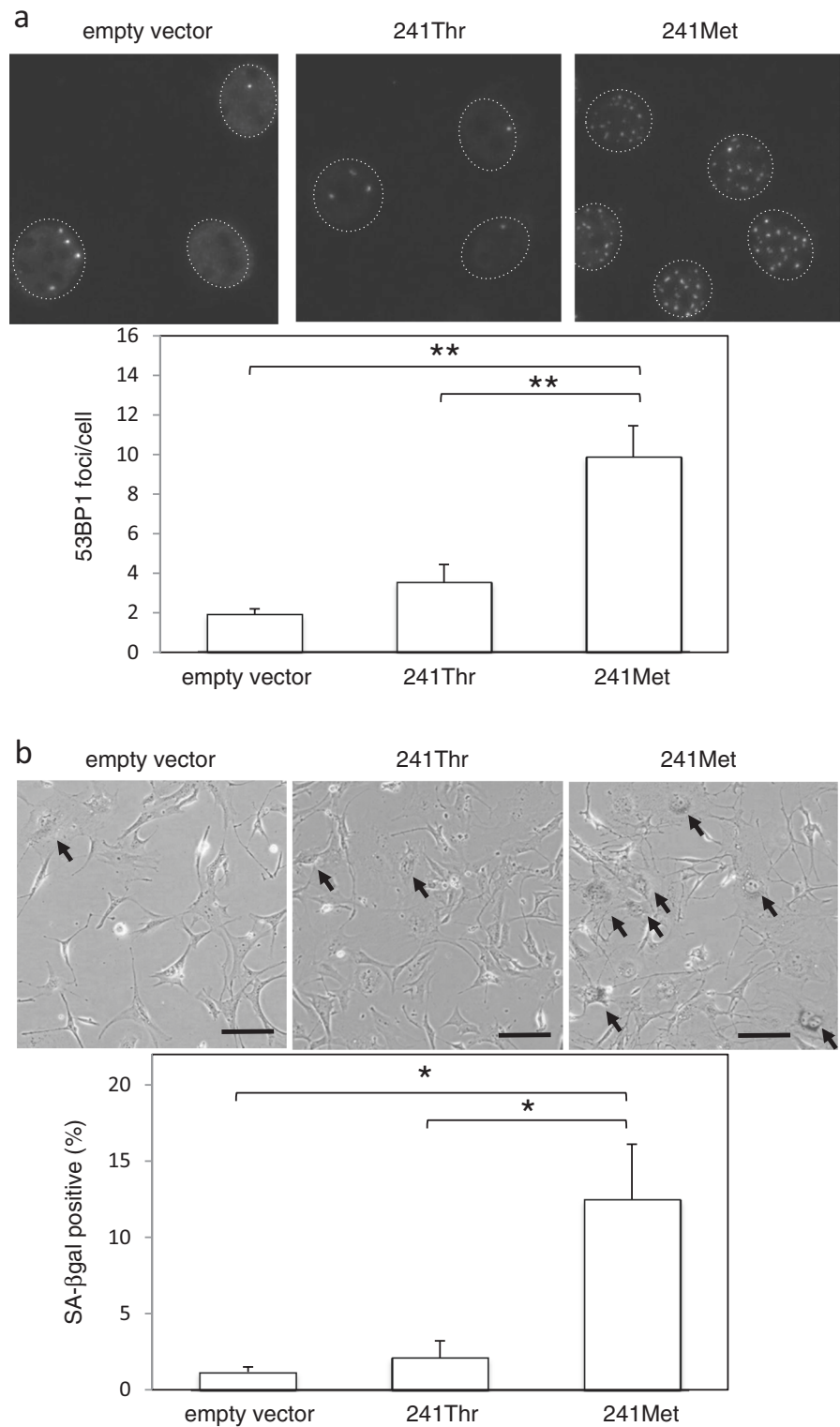
We next examined the phenotypic change of the cells in response to the introduction of the XRCC3 241Met variant. First, spontaneous DNA DSBs were determined by immunofluorescent study with anti-53BP1 antibody, because XRCC3 is a protein participating in DSBs repair pathway. Spontaneous DSBs accumulated to a greater degree in NIH3T3 cells expressing XRCC3 241Met (3T3-241Met) than in those expressing XRCC3 241Thr (3T3-241Thr) (Fig. 2a). Because DNA damage is known to be a mediator for cellular senescence [8], we tested whether cellular senescence induced by ionizing radiation is increased in 3T3-241Met. Consistent with the result of spontaneous DSBs, cellular senescence was induced to a greater degree in 3T3-241Met than in 3T3-241Thr (Fig. 2b).

As it is known that the inflammatory signaling molecules induce hypertrophic and fibrotic responses during hypertrophic remodeling, we evaluated the expression of the IL-6, IL-8, and MCP-1 genes in 3T3-241Thr and 3T3-241Met. MCP-1 mRNA levels were higher in 3T3-241Met than in

3T3-241Thr (Fig. 3a). However, there was no differences in IL-6 and IL-8 mRNA levels when comparing 3T3-241Thr and 3T3-241Met (Fig. 3a). Next, TNF- α stimulated expression of the IL-6, IL-8, and MCP-1 genes was examined in 3T3-241Thr and 3T3-241Met. TNF- α significantly increased the mRNA levels of IL-6 (3T3-241Thr, $p < 0.05$; 3T3-241Met, $p < 0.01$) and MCP-1 (all $p < 0.01$) (Fig. 3b), but not of IL-8 (data not shown). TNF- α stimulated expression of the MCP-1 gene was significantly increased in 3T3-241Met when compared with pMMTV or 3T3-241Thr, whereas that of IL-6 was not different when comparing 3T3-241Thr and 3T3-241Met (Fig. 3b). To confirm whether the increase in MCP-1 mRNA was followed by an increase in the protein level, secreted MCP-1 protein in culture medium from 3T3 cells with empty vector (3T3-empty), 3T3-241Thr, and 3T3-241Met was quantified by ELISA. The level of the secreted protein in 3T3-241Met was increased in basal condition compared with 3T3-empty or 3T3-241Thr (Supplementary Figure 2). TNF- α stimulation significantly increased MCP-1 protein secretion in 3T3-empty ($p < 0.01$), 3T3-241Thr ($p < 0.01$), and 3T3-241Met ($p < 0.01$), and the MCP-1 protein level is higher in the medium from 3T3-241Met than that from 3T3-empty or 3T3-241Thr (Supplementary Figure 2).

FACS was used to determine the effect of XRCC3 genotypes on the cell cycle and DNA content of NIH3T3

Fig. 2 Induction of XRCC3 241Met increases spontaneous DNA double-strand breaks and radiation-induced cellular senescence. NIH 3T3 cells were stably transfected either with pMMTV containing no insert (empty vector), 241Thr or 241Met. **a** NIH3T3 cells were serum-starved with 0.1% fetal calf serum (FCS)/Dulbecco's modified Eagles medium (DMEM) for 24 h, fixed and stained with anti-53BP1 antibody. All images of slides were obtained, and foci were counted automatically. Foci in approximately 4000 nuclei were counted. $**P < 0.01$. **b** Cells were irradiated at 7 Gy and maintained for 5 days in growth medium prior to Senescence-associated β -galactosidase (SA β -gal) staining (scale bars of 300 μ m). $*P < 0.05$. A full color version of this figure is available at the *Hypertension Research* journal online



cells. Representative images of cell cycle distribution are presented in Fig. 3c. Notably, 3T3-241Met showed a marked increase in polyploidy (Fig. 3c), whereas none of the 3T3-241Thr clones showed an increase in polyploidy. As summarized in Fig. 3d, the cell percentage in the G2/M

phase was significantly increased and G0/G1 phase was significantly decreased in 3T3-241Met when compared with 3T3-241Thr. The sum of the cell percentage in the G2/M phase and polyploidy was also significantly increased in 3T3-241Met when compared with 3T3-241Thr (pMMTV,

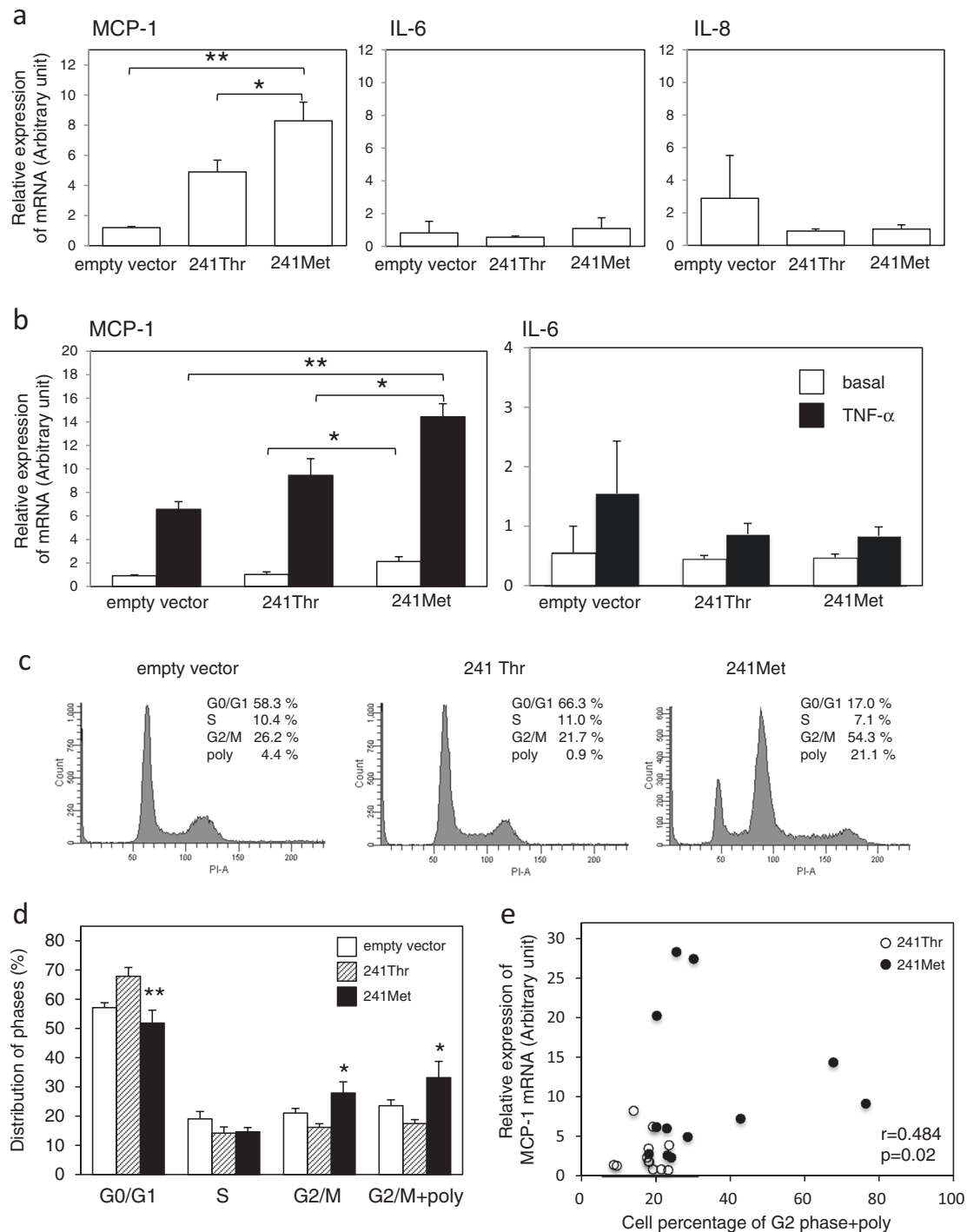


Fig. 3 Induction of XRCC3 241Met increases relative mRNA levels of MCP-1 and the cell percentages in the G2/M phase and polyploidy. NIH3T3 cells were stably transfected either with pMMTV containing no insert (empty vector), 241Thr or 241Met. **a** RNA was extracted and analyzed for the mRNA levels of MCP-1, interleukin (IL)-6, and IL-8 by quantitative real-time polymerase chain reaction (RT-PCR). * $P < 0.05$, ** $P < 0.01$. **b** Cells were serum-starved with 0.1% fetal calf serum (FCS)/Dulbecco's modified Eagles medium (DMEM) for 24 h and stimulated with 10 ng/mL tumor necrosis factor (TNF)- α for 24 h. RNA was extracted and analyzed for the mRNA levels of MCP-1, IL-6, and IL-8 by quantitative RT-PCR. * $P < 0.05$, ** $P < 0.01$. **c** The

cell cycle distribution was analyzed by fluorescence-activated cell sorting (FACS). Representative images of cell cycle distribution are shown. **d** Cell cycle distribution of NIH3T3 cells with pMMTV containing no insert (empty vector), 241Thr, or 241Met. Data are presented as the mean \pm standard error of the ten individual clones, and experiments were repeated three times. * $P < 0.05$, ** $P < 0.01$. **e** Relationship between cell percentage in the G2/M phase/polyploidy and relative levels of MCP-1 mRNA. Open circle represents NIH3T3 cells transfected with 241Thr, and closed circle represents those with 241Met. Data are presented for four individual clones, and experiments were repeated three times

$24 \pm 2\%$; 3T3-241Thr, $17 \pm 1\%$; 3T3-241Met, $33 \pm 6\%$). In addition, MCP-1 mRNA levels were positively correlated with the sum of the cell percentage in the G2/M phase and polyploidy (Fig. 3e). A similar correlation was observed between MCP-1 mRNA levels and the cell percentage in the G2/M phase (data not shown).

Discussion

Hypertension is the most common cause of LVH. However, not all hypertensive patients develop LVH, and the incidence of LVH does not solely depend on the duration or severity of hypertension [1]. The present study sought to determine whether genetic factors, especially XRCC3 polymorphism, affect the incidence of hypertension-induced LVH and to elucidate any underlying mechanisms. The principal findings were: (1) there was a significant difference in genotype distribution ($\chi^2 = 7.85$, $p = 0.0051$) and allele frequency distribution ($\chi^2 = 6.80$, $p = 0.009$) between the LVH(+) group and the LVH(−) group in patients who were undergoing HD; (2) the risk of LVH was higher in XRCC3 241Thr/Met patients than in XRCC3 241Thr/Thr patients; (3) in vitro experiments revealed that XRCC3 241Met increased spontaneous DNA damage, arrest of cells at the G2/M checkpoint, polyploidy, and cell size, and induced a proinflammatory phenotype in cells. This is the first report to show the association between XRCC3 polymorphism and LVH susceptibility and to examine its possible mechanisms.

A single nucleotide polymorphism in exon 7 of the XRCC3 gene results in the amino acid change (threonine to methionine) at codon 241. As XRCC3 is one of the proteins responsible for repairing DNA DSBs, a number of studies have been conducted to clarify the association between XRCC3 Thr241Met polymorphism and cancer susceptibility [9–11]. We previously reported that XRCC3 deficiency or the XRCC3 241Met variant results in increased endoreduplication and polyploidy [3]. Polyploidy results in increased cell size and increase body size in plants and animals [12]. Engelmann et al. reported that spontaneously hypertensive rats (SHR) have greater cardiac mass than Wistar–Kyoto rats (WKY) and that LV cardiac myocytes from SHR show significantly more polyploidy than those from WKY [13]. Thus, we examined whether XRCC3 polymorphism is associated with LVH. We found that CHO-K1 cells transfected with XRCC3 241Met were larger than those with XRCC3 241Thr. In addition, XRCC3 241Met accelerated the transition of the NIH3T3 cells from the G0/G1 phase (2n) into the G2/M phase (4n) and increased the cellular population with polyploidy (8n). These findings suggest that the XRCC3 241Met variant arrests the cells at the G2/M checkpoint or inhibits

cytokinesis, thereby increasing the DNA content of the cells and inducing cell hypertrophy.

Non-cardiomyocytes play a pivotal role in the development of cardiac hypertrophy. Inflammatory cytokines, such as IL-6, MCP-1, TNF- α , and transforming growth factor (TGF)- β , and neurohormonal factors, such as angiotensin II, secreted from non-cardiomyocytes are involved in the pathophysiology and progression of hypertrophy [14, 15]. We examined the expression of inflammatory cytokines in NIH3T3 cells with 241Thr or 241Met and found that MCP-1 mRNA levels were higher in NIH3T3 cells transfected with the 241Met variant than those with 241Thr, both in the basal state and in response to TNF- α . Kuwahara et al. showed that inhibition of MCP-1 with neutralizing antibodies significantly reduced macrophage accumulation and attenuated myocardial fibrosis in rat LVH that was induced by suprarenal aortic constriction [16]. Our data suggest that the XRCC3 241Met variant induces an inflammatory phenotype and secretion of MCP-1 in fibroblasts, which plays an important role in cardiac fibrosis and the development of LVH.

In our study, FACS analysis revealed that the cell percentage in the G2 phase, including polyploid cells, was significantly increased in NIH3T3 cells transfected with XRCC3 241Met when compared with 241Thr. In addition, susceptibility to senescence by radiation-induced DNA damage increased in XRCC3 241Met clones when compared with 241Thr clones. These results are consistent with a recent report from Nakanishi and other researchers. They showed that mitosis skip, which results in polyploidation, and sustained G2 arrest are necessary and sufficient for the induction of senescence [12, 17, 18]. Furthermore, there is growing evidence that DNA damage and DNA damage response induces cellular senescence and that a trait of cellular senescence is the acquisition of a senescence-associated secretory phenotype (SASP), which entails a substantial increase in the secretion of proinflammatory cytokines and chemokines [8]. In our study, spontaneous DNA damage and expression of MCP-1 was increased in NIH3T3 cells with XRCC3 241Met. Further, MCP-1 mRNA levels were positively correlated with sum of the cell percentage in the G2/M phase and polyploidy. Taken together, our findings suggest that the XRCC3 241Met variant induces cellular senescence via sustained G2 arrest, which results in acquisition of a proinflammatory phenotype.

Our study has several limitations. First, we included hypertensive patients undergoing chronic HD in this study because they show continuous high blood pressure due to pressure overload and volume overload. However, as hypertension in the HD patients is multifactorial, the current results may not apply to non-HD patients with essential hypertension-induced LVH. Second, we conducted our

in vitro experiments with CHO cells and NIH3T3 fibroblasts because transfection efficiency is comparatively lower in cardiac cells. Further studies are required to elucidate the role of the XRCC3 241Met allele in cardiomyocytes and cardiac fibroblasts.

Acknowledgements We thank Dr. Oren Traub for editing this manuscript. Part of this work was performed at the Analysis Center of Life Science, Natural Science Center for Basic Research and Development, and the Joint Usage/Research Center (RIRBM), Hiroshima University. This work was supported by Grants-in-Aid for Scientific Research from the Ministry of Education, Culture, Sports, Science and Technology of Japan (KAKENHI#15K09122 to MI and KAKENHI#17K10449 to TI), research grants from the Takeda Science Foundation (<http://www.takeda-sci.or.jp/index.html>) to MI, the SENSHIN Medical Research Foundation (<http://www.mt-pharma.co.jp/zaidan/>) to MI and the program of the network-type joint Usage/Research Center for Radiation Disaster Medical Science of Hiroshima University, Nagasaki University, and Fukushima Medical University. Dr. Ariyandy was financially supported by the Directorate General of Resources for Research, Technology & Higher Education (DG-RSTHE), Indonesia.

Compliance with ethical standards

Conflict of interest The authors declare that they have no conflict of interest.

References

- Katholi RE, Couri DM. Left ventricular hypertrophy: major risk factor in patients with hypertension: update and practical clinical applications. *Int J Hypertens*. 2011;2011:495349.
- Bella JN, Goring HH. Genetic epidemiology of left ventricular hypertrophy. *Am J Cardiovasc Dis*. 2012;2:267–78.
- Yoshihara T, Ishida M, Kinomura A, Katsura M, Tsuruga T, Tashiro S, Asahara T, Miyagawa K. XRCC3 deficiency results in a defect in recombination and increased endoreduplication in human cells. *EMBO J*. 2004;23:670–80.
- David-Beabes GL, Lunn RM, London SJ. No association between the XPD (Lys751Gln) polymorphism or the XRCC3 (Thr241Met) polymorphism and lung cancer risk. *Cancer Epidemiol Biomark Prev*. 2001;10:911–2.
- McFarland TM, Alam M, Goldstein S, Pickard SD, Stein PD. Echocardiographic diagnosis of left ventricular hypertrophy. *Circulation*. 1978;57:1140–4.
- Wanner C, Amann K, Shoji T. The heart and vascular system in dialysis. *Lancet*. 2016;388:276–84.
- Ok E, Asci G, Chazot C, Ozkahya M, Mees EJ. Controversies and problems of volume control and hypertension in haemodialysis. *Lancet*. 2016;388:185–93.
- Watanabe S, Kawamoto S, Ohtani N, Hara E. Impact of senescence-associated secretory phenotype and its potential as a therapeutic target for senescence-associated diseases. *Cancer Sci*. 2017;108:563–9.
- Bei L, Xiao-Dong T, Yu-Fang G, Jian-Ping S, Zhao-Yu Y. DNA repair gene XRCC3 Thr241Met polymorphisms and lung cancer risk: a meta-analysis. *Bull Cancer*. 2015;102:332–9.
- Perez-Ramirez C, Canadas-Garre M, Molina MA, Robles AI, Faus-Dader MJ, Calleja-Hernandez MA. Contribution of genetic factors to platinum-based chemotherapy sensitivity and prognosis of non-small cell lung cancer. *Mutat Res*. 2017;771:32–58.
- Qin XP, Zhou Y, Chen Y, Li NN, Wu XT. XRCC3 Thr241Met polymorphism and gastric cancer susceptibility: a meta-analysis. *Clin Res Hepatol Gastroenterol*. 2014;38:226–34.
- Johmura Y, Shimada M, Misaki T, Naiki-Ito A, Miyoshi H, Motoyama N, Ohtani N, Hara E, Nakamura M, Morita A, Takahashi S, Nakanishi M. Necessary and sufficient role for a mitosis skip in senescence induction. *Mol Cell*. 2014;55:73–84.
- Engelmann GL, Vitullo JC, Gerrity RG. Age-related changes in ploidy levels and biochemical parameters in cardiac myocytes isolated from spontaneously hypertensive rats. *Circ Res*. 1986;58:137–47.
- Frieler RA, Mortensen RM. Immune cell and other non-cardiomyocyte regulation of cardiac hypertrophy and remodeling. *Circulation*. 2015;131:1019–30.
- van Vuren EJ, Malan L, von Kanel R, Cockeran M, Malan NT. Hyperpulsatile pressure, systemic inflammation and cardiac stress are associated with cardiac wall remodeling in an African male cohort: the SABPA study. *Hypertens Res*. 2016;39:648–53.
- Kuwahara F, Kai H, Tokuda K, Takeya M, Takeshita A, Egashira K, Imaizumi T. Hypertensive myocardial fibrosis and diastolic dysfunction: another model of inflammation? *Hypertension*. 2004;43:739–45.
- Johmura Y, Yamashita E, Shimada M, Nakanishi K, Nakanishi M. Defective DNA repair increases susceptibility to senescence through extension of Chk1-mediated G2 checkpoint activation. *Sci Rep*. 2016;6:31194.
- Nakayama Y, Yamaguchi N. Role of cyclin B1 levels in DNA damage and DNA damage-induced senescence. *Int Rev Cell Mol Biol*. 2013;305:303–37.